

Electronic Supplementary Information

Hydrophobic pocket targeting probe for enteroviruses

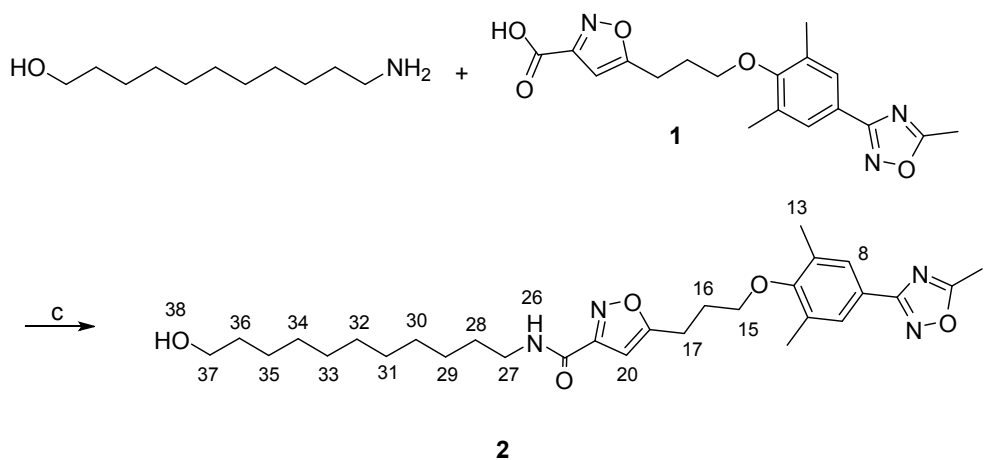
*Mari Martikainen^{a,d}, Kirsi Salorinne^{b,d}, Tanja Lahtinen^{b,d}, Sami Malola^{c,d}, Perttu Permi^{a,b,d,e},
Hannu Häkkinen^{b,c,d*} and Varpu Marjomäki^{a,d*}*

Departments of ^aBiology and Environmental Science, ^bChemistry, and ^cPhysics, and
^dNanoscience Center, University of Jyväskylä, FI-40014 Jyväskylä, Finland;
^eInstitute of Biotechnology, University of Helsinki, FI-00014 Helsinki, Finland

Experimental

General. All reagents were commercial and used as received unless otherwise mentioned. Dichloromethane was distilled over CaCl₂ and stored over 3Å molecular sieves under N₂-atmosphere. 11-Amino-1-undecanol¹, compound **1**², and Au₁₀₂(pMBA)₄₄ cluster³ were prepared according to previously published procedures. Azadioxatriangulenium dye^{4,5} was obtained as a courtesy of Thomas Just Sørensen and Bo W. Larsen from the University of Copenhagen. ¹H and ¹³C NMR spectra were recorded with Bruker Avance 300 or 400 MHz spectrometers and chemical shifts were calibrated to the residual proton or carbon resonance of the solvent. Accurate HRMS spectra were measured with Micromass LCT ESI-TOF mass spectrometer using Leucine Enkephalin as an internal calibration. Melting points were determined with Stuart SMP3 melting point apparatus in open capillaries. Gel electrophoresis visualization was run on 15% polyacrylamide gel (29:1, acrylamide:bisacrylamide) using 1X TBE buffer in a Bio-Rad Mini-Protean Tetra System gel electrophoresis apparatus at 130 V for 2 hours. UV/Vis spectra were measured with Perkin Elmer Lambda 850 spectrometer. IR-spectra were measured with Perkin Elmer Tensor 27 FTIR-spectrometer using diamond ATR.

Synthesis of the probe (2)



Scheme S1. Synthesis protocol for the probe (2): (A) potassium phthalimide, DMF, 80°C, (B) hydrazine monohydrate, ethanol, 0°C → reflux, (C) EDC, HOBt, DCM, 0°C → RT. Numbering scheme for proton NMR assignment is shown.

5-(3-(2,6-dimethyl-4-(5-methyl-1,2,4-oxadiazol-3-yl)phenoxy)propyl)-N-(11-

hydroxyundecyl)-isoxazole-3-carboxamide (2): A solution of 1 (0.062 g, 0.17 mmol) in dry dichloromethane (20 mL) in a round-bottomed flask equipped with a CaCl₂-tube was cooled to 0°C in an ice-bath with stirring. EDC (34 μL, 0.19 mmol) was added followed by 1-hydroxybenzotriazole monohydrate (0.026 g, 0.19 mmol) and the reaction mixture was stirred at 0°C for about one hour before the addition of solid 11-amino-1-undecanol (0.029 g, 0.18 mmol) in one portion. The reaction mixture was allowed to warm to RT and stirred overnight to complete the reaction. The reaction mixture was then poured into a separatory funnel and washed successively with 2 N hydrogen chloride solution, saturated aqueous NaHCO₃ solution, water and brine. The organic layer was collected, dried with anhydrous Na₂SO₄ and solvent was removed by rotavapor. Chromatographic purification by CombiFlash Companion in silica with dichloromethane-methanol 95:5 provided the title compound after recrystallization from methanol-water as white crystalline solid. Yield 0.062 g (68 %). m.p. 92–94 °C. ¹H NMR (CDCl₃, 400 MHz): δ_H = 7.72 (s, 2H, H-8), 6.78 (t, 1H, *J* = 5.67 Hz, NH-26), 6.52 (s, 1H, H-20), 3.87 (t, 2H, *J* = 6.00 Hz, H-15), 3.64 (t, 2H, *J* = 6.60 Hz, H-37), 3.42 (q, 2H, *J* = 6.96 Hz, H-27), 3.11 (t, 2H, *J* = 7.52 Hz, H-17), 2.64 (s, 3H, H-1), 2.31 (s, 6H, H-13), 2.24 (q, 2H, *J* = 7.24 Hz, H-16), 1.58 (m, 4H, H-36 and H-28), 1.28 (m, 14H, H-29 – H-35) ppm. ¹³C NMR (CDCl₃, 100 MHz): δ_C = 176.3, 174.5, 168.1, 160.0, 158.8, 158.2, 131.6, 128.1, 122.3, 100.9, 70.4, 63.1, 39.5, 32.8, 29.5, 29.4, 29.3, 29.2, 28.3, 26.8, 25.7, 23.6, 16.3, 16.2, 12.4 ppm. HRMS (ESI-TOF) *m/z*: 549.3046 [M – Na⁺], required 549.3047.

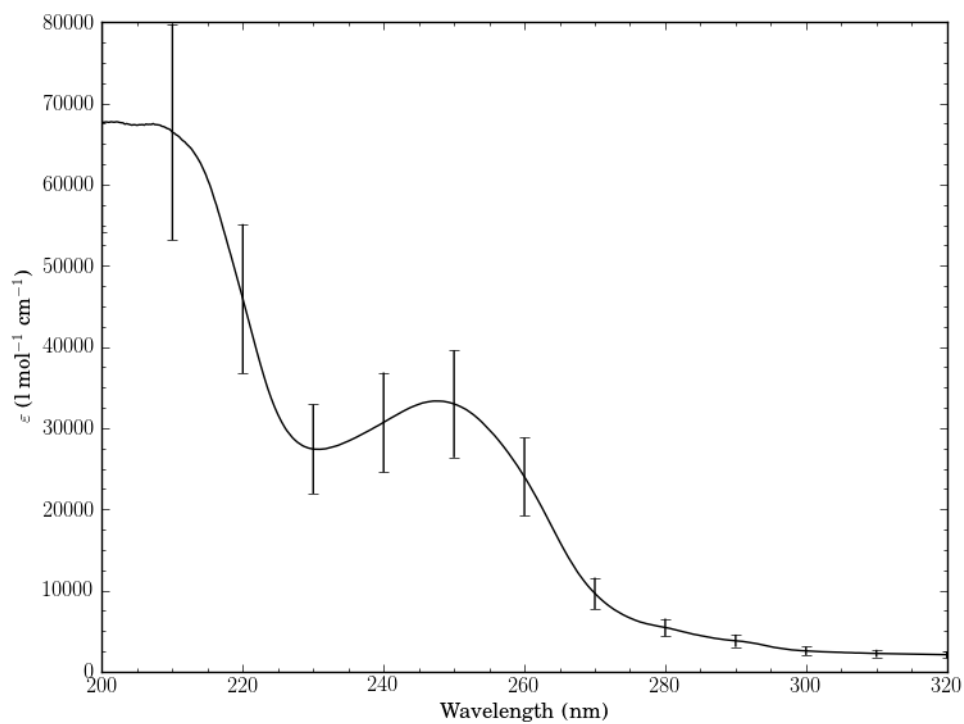


Figure S1. UV/Vis absorption coefficient of probe (2).

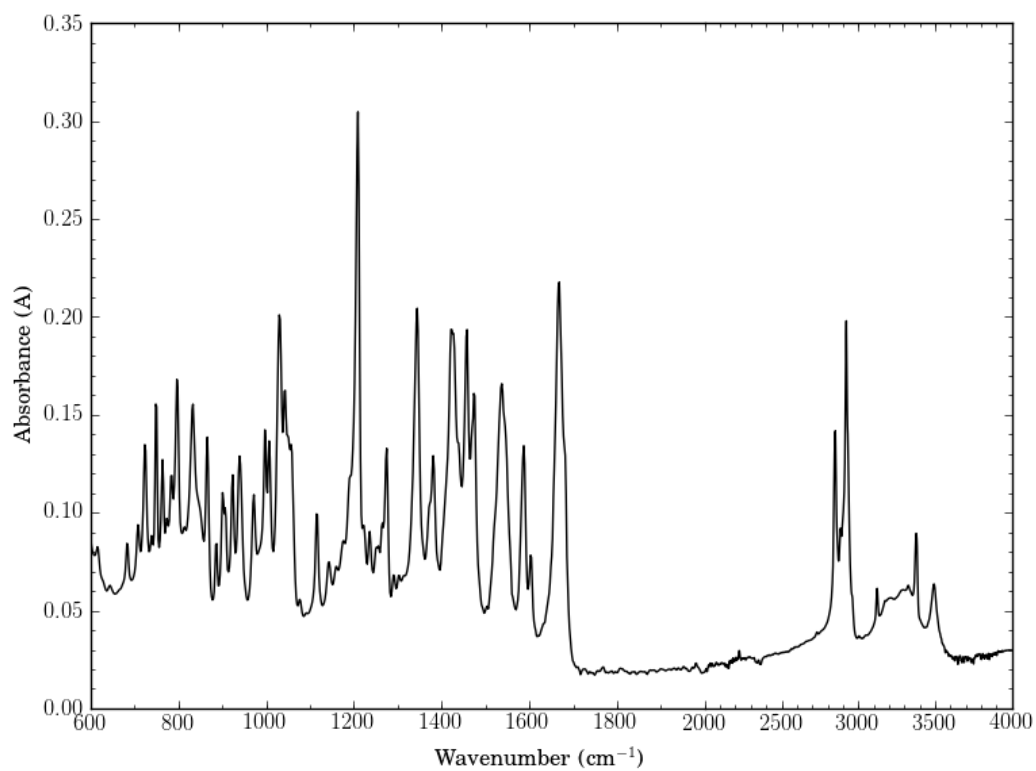
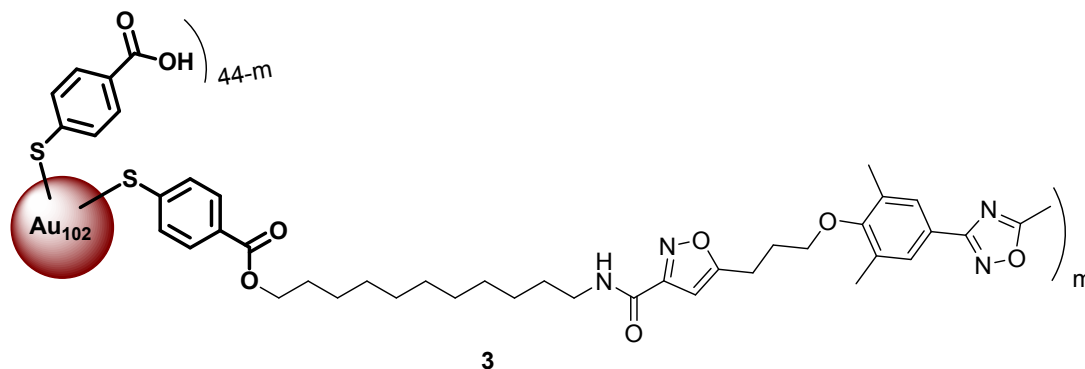


Figure S2. FTIR-ATR spectrum of probe (2).

Synthesis of gold cluster labeled probe (**3**)



Scheme S2. Synthesis protocol for $\text{Au}_{102}(\text{pMBA})_{44}$ cluster labeled probe (**3**): $\text{Au}_{102}(\text{pMBA})_{44}$, **2**, DCC, DMSO, $0^\circ\text{C} \rightarrow \text{RT}$.

A solution of **2** (2.0 mg, 4.01 μmol) in dry DCM (1 mL) was added to a pre-sonicated solution of $\text{Au}_{102}(\text{pMBA})_{44}$ (2.0 mg, 0.0745 μmol) in dry DMSO (5 mL) in a 25-mL round-bottom flask. The reaction mixture was vigorously stirred for 20 minutes at RT. After this, a solution of N,N'-dicyclohexylcarbodiimide (0.77 mg, 3.73 μmol) in dry DCM (1 mL) was added dropwise to the cooled reaction mixture on an ice-bath while stirring. The reaction mixture was then allowed to warm to RT and continued to stir overnight. After this, the reaction mixture was centrifuged at 3500 rpm for 5 min. Supernatant was collected and transferred to a new 50-mL conical and the functionalized nanoparticles **3** were precipitated from the solution by adding NH_4OAc (73mg, 0.82 mmol) and MeOH (20 mL). The conical was shaken to mix all the contents and then centrifuged at 3500 rpm for 15 min. The precipitates were collected, dried and dissolved in ultrapure water. Gel electrophoresis visualization was run on 15% polyacrylamide gel (29:1) at 130 V for 2 hours.

Success of the functionalization was seen as multiple bands in the polyacrylamide gel (Figure S3a). The distinctive brown color of Au_{102} -clusters arising from the size of the gold core remained unchanged in the probe (**2**) functionalized Au_{102} -clusters (**3**), which indicated that the gold core was unaffected by the functionalization. This was also confirmed by UV-Vis analysis (Figure S3b).

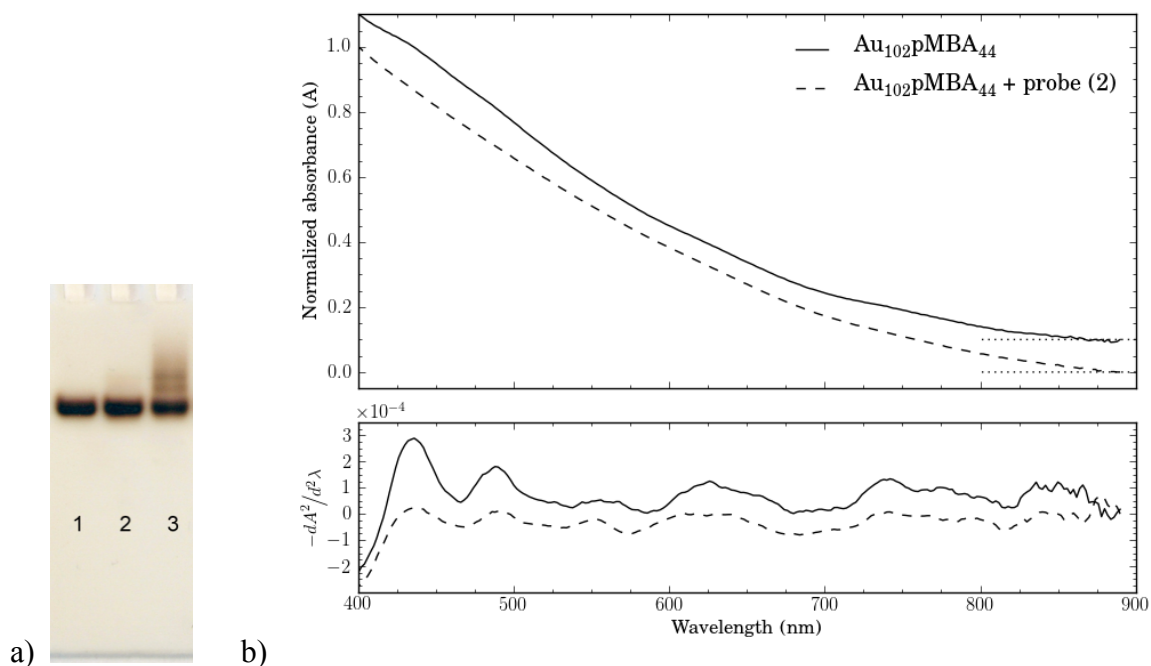
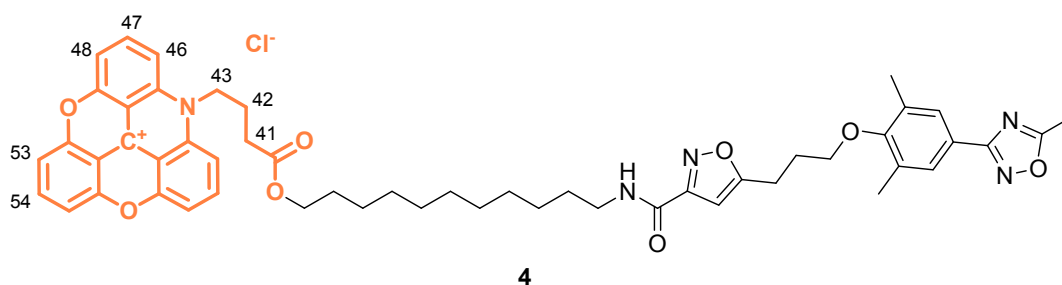


Figure S3. A) 15% PAGE (29:1) analysis showing unfunctionalized $\text{Au}_{102}(\text{pMBA})_{44}$ clusters (lane 1) and probe-2 functionalized $\text{Au}_{102}(\text{pMBA})_{44}$ clusters **3** (lane 3). Most of the unfunctionalized $\text{Au}_{102}(\text{pMBA})_{44}$ clusters precipitate from the reaction mixture and are separated out during the first centrifugation (lane 2) leaving the probe-2 functionalized gold clusters in the supernatant. B) UV-Vis spectrum of pure and functionalized $\text{Au}_{102}\text{pMBA}_{44}$. The spectrum is similar before and after the functionalization, indicating that the cluster core has remained intact.

Synthesis of fluorescent dye labeled probe (**4**)



Scheme S3. Synthesis protocol for the fluorescent dye labeled probe (**4**): Carboxylic acid derivative of azadioxatriangulenium dye, **2**, DCC, DMAP, DCM-DMSO, $0^{\circ}\text{C} \rightarrow \text{RT}$. Numbering scheme for proton NMR assignment is shown for the dye moiety, see scheme S1 for KIRTAN-1 assignment.

Carboxylic acid derivative of azadioxatriangulenium dye^{4,5} (2.5 mg, 5.6 μmol) was first dissolved in a small amount of dry DMSO (0.2 mL) and then added to a stirred dry dichloromethane (5 mL) in a round-bottom flask equipped with a CaCl_2 -tube at RT. Probe (**2**) (5.9 mg, 11.0 μmol) and DMAP (0.4 mg, 3.4 μmol) were added subsequently and the reaction mixture was cooled to 0°C in an ice-bath. Solid DCC (1.4 mg, 6.8 μmol) was added

in one portion and the reaction mixture was continued to stir at 0°C for additional 5 minutes and then allowed to warm to RT and stirred for 23 hours. The reaction mixture was diluted with dichloromethane and washed two times with 0.5 N hydrogen chloride solution and two times with saturated aqueous NaHCO₃ solution. The organic layer was collected, dried with anhydrous Na₂SO₄ and solvent was removed by rotavapor. Purification by flash chromatography on silica eluting with a mixture of dichloromethane-methanol (9:1) gave the product as red solid. Yield 3.6 mg (26 %). ¹H NMR (CDCl₃, 300 MHz): δ_H = 8.62 (br d, 2H, *J* = 7.74 Hz, H-46), 8.44 (br t, 2H, *J* = 15.46 Hz, H-47), 8.02 (t, 1H, *J* = 8.48 Hz, H-54), 7.71 (t, 2H, *J* = 0.56 Hz, H-8), 7.50 (d, 2H, *J* = 7.95 Hz, H-48), 7.42 (d, 2H, *J* = 8.42 Hz, H-53), 6.82 (br t, 1H, *J* = 6.35 Hz, NH-26), 6.53 (s, 1H, H-20), 5.22 (br t, 2H, H-43), 4.13 (t, 2H, *J* = 6.75 Hz, H-37), 3.86 (t, 2H, *J* = 6.05 Hz, H-15), 3.43 (q, 2H, *J* = 6.81 Hz, H-27), 3.10 (t, 2H, *J* = 7.81 Hz, H-17), 3.01 (br t, 2H, H-41), 2.64 (s, 3H, H-1), 2.30 (s, 6H, H-13), 2.23 (m, 4H, H-42 and H-16), 1.57 (m, 4H, H-36 and H-28), 1.30 (m, 14H, H-29 – H-35) ppm.

STD and trNOESY NMR Experiments

STD and trNOESY NMR experiments were acquired with a Varian Inova 800 MHz spectrometer equipped with a cryogenically cooled ¹H, ¹³C, ¹⁵N triple-resonance z-axis gradient probehead. Echovirus 1 (EV1) sample was prepared as 20 nM solution in 2 mM MgCl₂-PBS buffer in D₂O by repeated dialysis. Amount of 1 μL of 25 mM solution of carboxylic acid derivative **1** in DMSO-d₆ was added to the EV1 sample, which gave the ligand concentration of about 100 μM and 5000-fold molar excess (83:1) with regards to EV1 binding sites. 5 mm Shigemi NMR tubes were used and ¹H NMR reference spectra of EV1 in D₂O buffer, ligand **1** in D₂O and EV1 + ligand **1** in D₂O buffer were measured at 25 °C. STD NMR spectra were recorded with 1 - 3.5 s saturation times at 20 ppm (reference spectrum) and -0.5 ppm (saturation transfer to ligand) regions. Difference spectra of these two experiments gave the STD NMR spectrum (see main text, Figure 1a). trNOESY spectrum was recorded with a 100 ms mixing time (Figure S4).

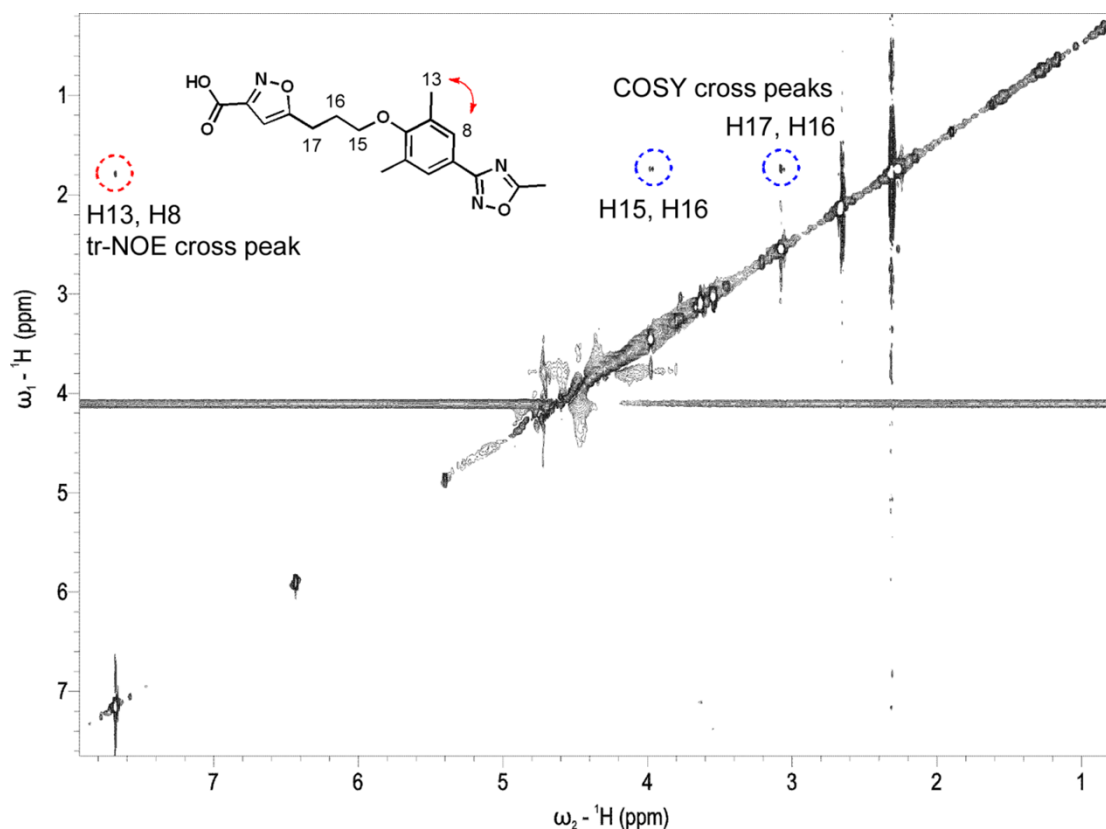


Figure S4. tr-NOESY NMR spectrum of EV1 virus particle and carboxylic acid derivative (**1**) in D₂O at 37°C. tr-NOE cross peak highlighted by red is observed between the aromatic ring protons H13 and H8 of derivative (**1**) due to binding to EV1. COSY cross peaks between the propoxy unit protons H17, H16 and H15 are marked with blue.

Determination of cytotoxicity

Cytotoxicity of the compounds in cell culture was determined in a 3-(4,5-dimethylthiazol-2-yl)-2,5-diphenyltetrazolium bromide (MTT) assay. The A549 cells were seeded at 1×10^4 cells per well in 96-well cell culture plate and grown for 48 h. Culture media was removed and cells treated with the compounds at different concentrations (10 and 25 $\mu\text{g}/\text{ml}$) in cell culture media (1 % FBS) for 48 h. Culture media was removed and 100 μl of 5 mg/ml MTT reagent (Millipore) in phenyl-red free medium added and incubated for 3 h at +37°C. Formed formazan crystals were dissolved with 100 μl of 0.04 N HCl in isopropanol. The optical density (OD) was measured at 570 nm using Victor™ X4 2030 Multilabel Reader (Perkin Elmer). Cell viability of individual compound-treated wells was evaluated as the percentage of the mean value of optical density resulting from six cell controls which was set 100% (Figure S5D).

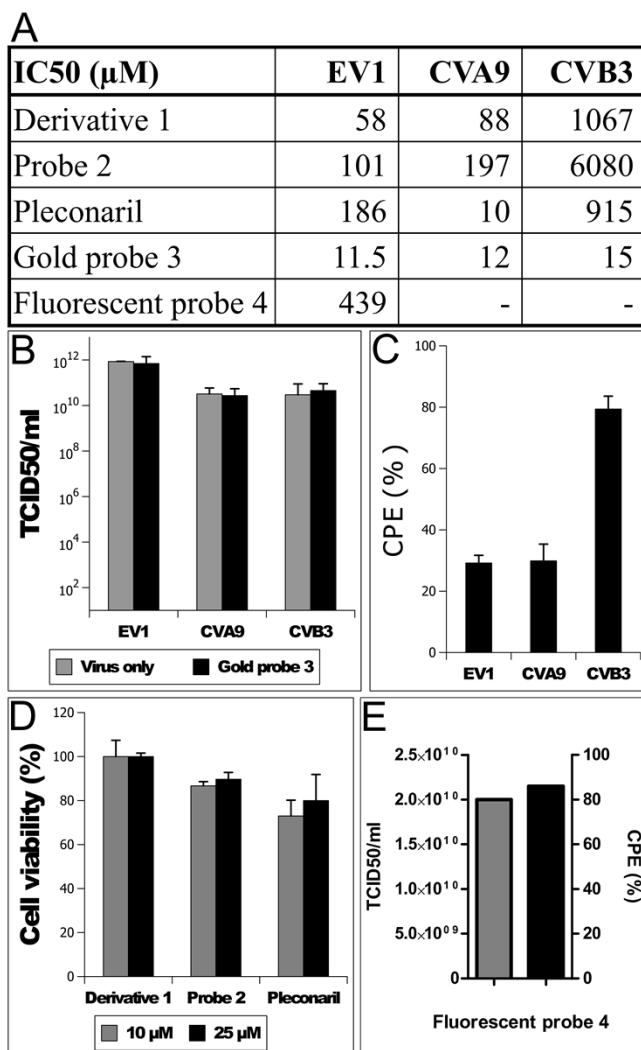


Figure S5. A) IC₅₀ values (μM) of studied compounds quantified with 24h CPE inhibition assay. B) TCID₅₀/ml values for viruses with gold probe (3). Infectivities were not affected. C) CPE inhibition assay for the gold probe (3) with studied viruses quantified with 24h CPE inhibition assay. Virus only was set to 100 % CPE and cells only to 0 % CPE. D) Cytotoxicity of the studied compounds after 48h on A549 cells. The studied concentrations of were not toxic to the cells. E) TCID₅₀/ml and CPE values for the fluorescent probe (4).

Cell Titer Glo assay

To summarize, the experiments were carried out using 2-day-old A549 cells (8×10^4 cells/well) in 96-well cell culture plates. The cell culture media was changed to fresh DMEM (containing 1% FBS). Cells were infected with MOI 5 in all wells. Viruses were pre-incubated for 1 h at 37°C with the studied compounds before the assay. For CPE-assay, 100 μM concentrations were used with all of the studied compounds during pre-incubation, and then compounds were diluted ten-fold when added on cells with the virus. Infected cells without the test compounds and non-infected cells served as virus only control (vc) and cell

control (cc), respectively. After 24 h, the viability of the cells was measured by quantifying the amount of ATP in cells using Cell Titer Glo (CTG) assay according to manufacturer's instructions (Promega). After infection, CTG was added on wells and the Luminescence was measured with the Victor™ X4 2030 Multilabel Reader according to the manufacturer's protocol. CPE values were calculated using following equation:

$\% \text{ CPE} = 100 - ([\text{OD}_{\text{virus}} + \text{compound}} - \text{OD}_{\text{vc}}] / \text{OD}_{\text{cc}}) \times 100$. Virus only controls were set to 100 % CPE and cells only controls to 0 %.

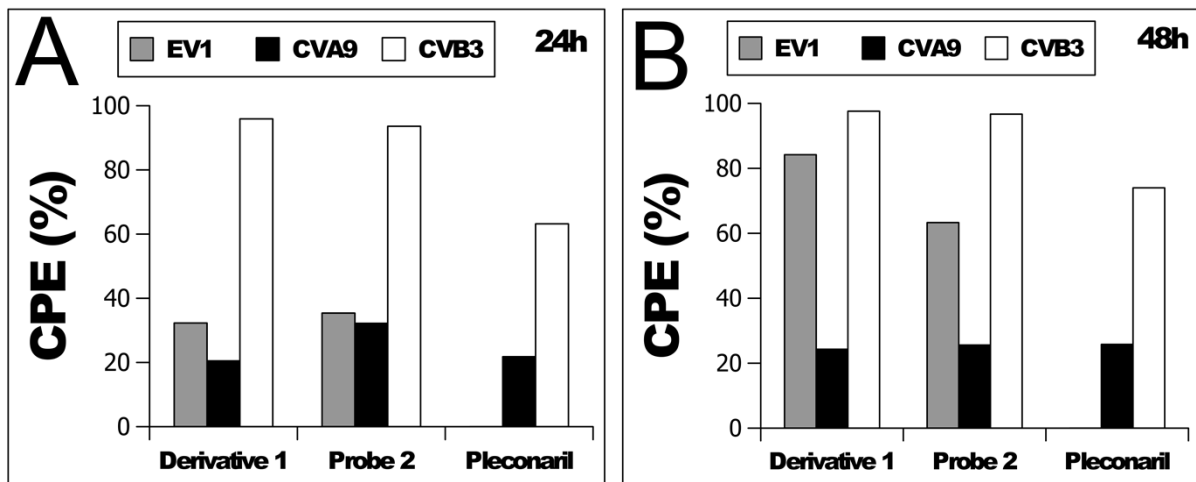


Figure S6. The effects of derivative (1), probe (2) and Pleconaril on CPE assay after A) 24 h and B) 48 h of infection quantified by Cell Titer Glo assay. A) At 24 h p.i. all three compounds had inhibitory effect on the infectivity of EV1 and CVA9. All the compounds had least effect on CVB3 infectivity which showed strong CPE on cells. B) At 48 h p.i. derivative (1) and probe (2) showed lower inhibitory effect on CPE for EV1 or CVB3 while the effect on CVA9 was still similar to the earlier time point. Virus only control was set to 100 % CPE and cells only control to 0 % CPE.

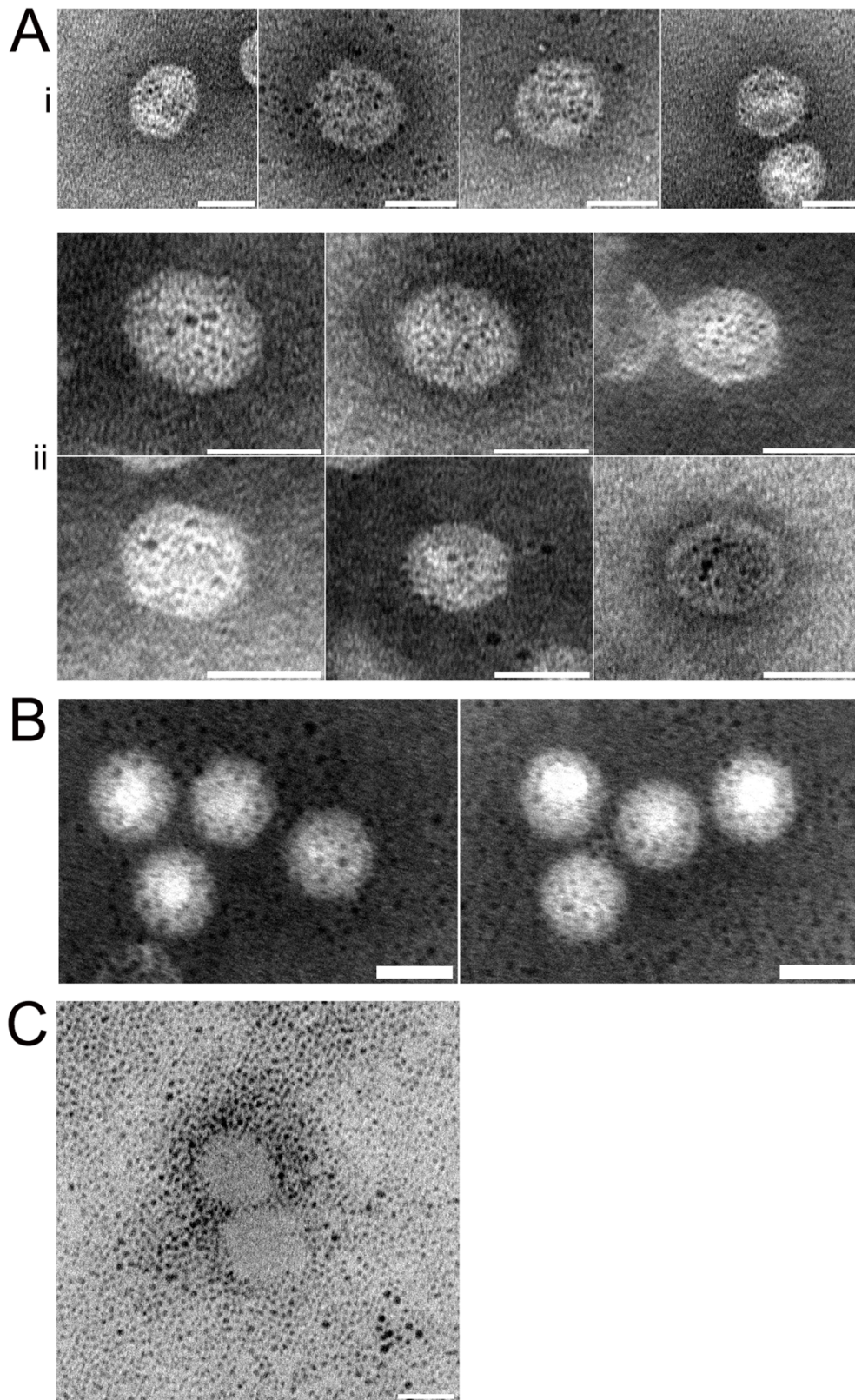


Figure S7. TEM micrographs of gold probe (**3**) conjugated to studied viruses. A) EV1-gold probe conjugates. Gold probes (**3**) are adhered to the virus capsid forming pentamer-like symmetries. i) Before column purification. ii) After the column purification. B) CVA9-gold probe conjugates. C) CVB3-gold probe conjugates. Gold probes (**3**) are seen around the virus and not bound to the capsid. Scale bars 20 nm.

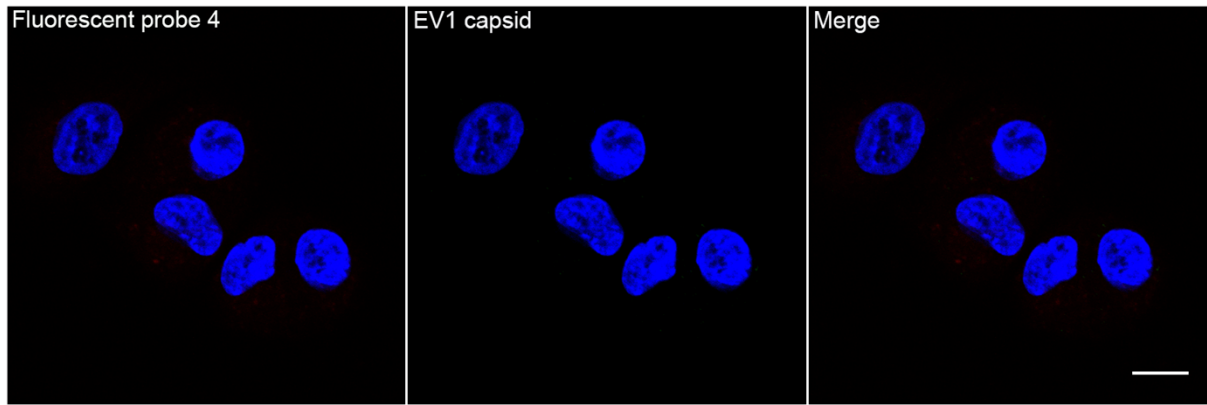


Figure S8. Uninfected control A549 cells. Fluorescent probe (4) only was internalized into cells. There was no significant background seen in the fixed samples. Scale bar 10 μ m.

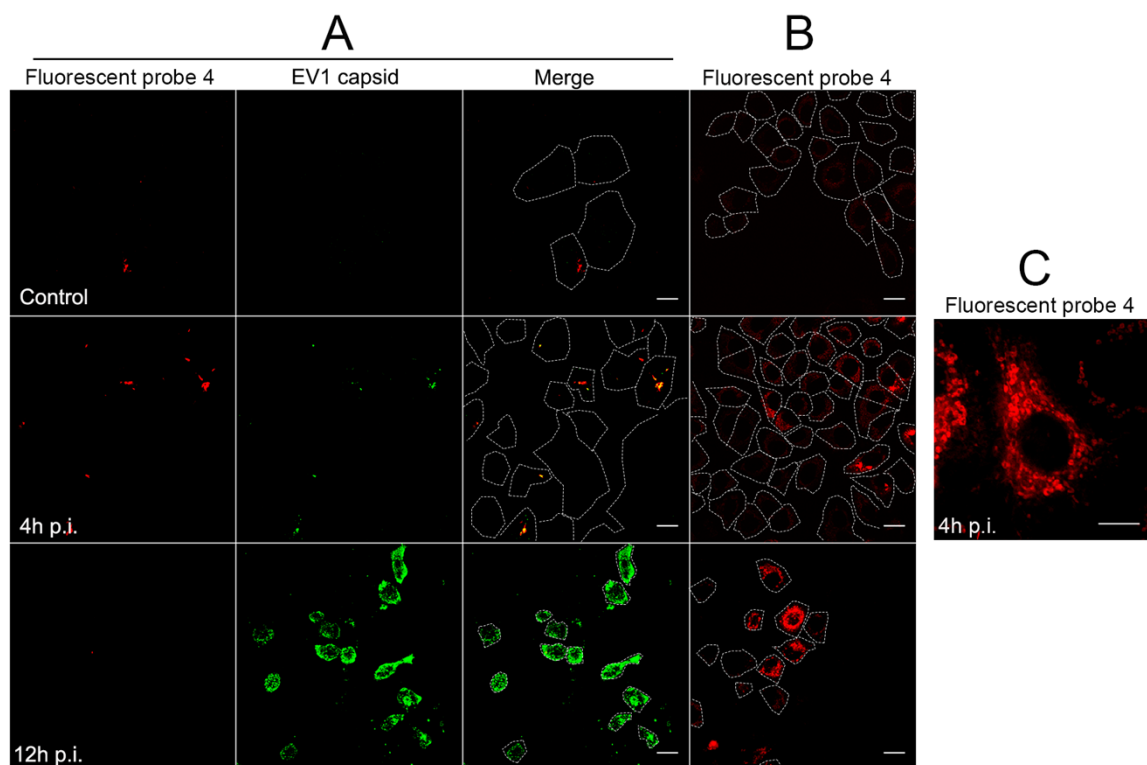


Figure S9. Live cell experiment with the fluorescent probe (4) conjugated to virus. A549 cells were infected with fluorescent probe-EV1 conjugate and imaged at different time points. After the live imaging, samples were fixed and the major capsid proteins of EV1 were labeled with capsid antibodies (green) to see if the fluorescent probe (4) colocalized in the same vesicular structures as where the virus capsid label resided. A) Fixed and labeled cells showed at 4 h p.i. the virus-fluorescent probe conjugate in the same vesicular structures as where the virus capsid label resided. At 12 h p.i., cells were showing high amounts of newly-synthesized viral capsid protein indicating successful infection. Scale bars, 10 μ m. B) Live imaging of virus-fluorescent probe conjugates showed bright vesicular structures in the cell cytoplasm at 4 and 12 h p.i.. In uninfected control cells the fluorescent probe (4) signal showed negligible signal and thus very low non-specific binding to cells. C) A close-up of a A549 cell at 4h p.i. showing vesicular structures full of fluorescent probe-EV1 conjugate. Scale bars 10 μ m.

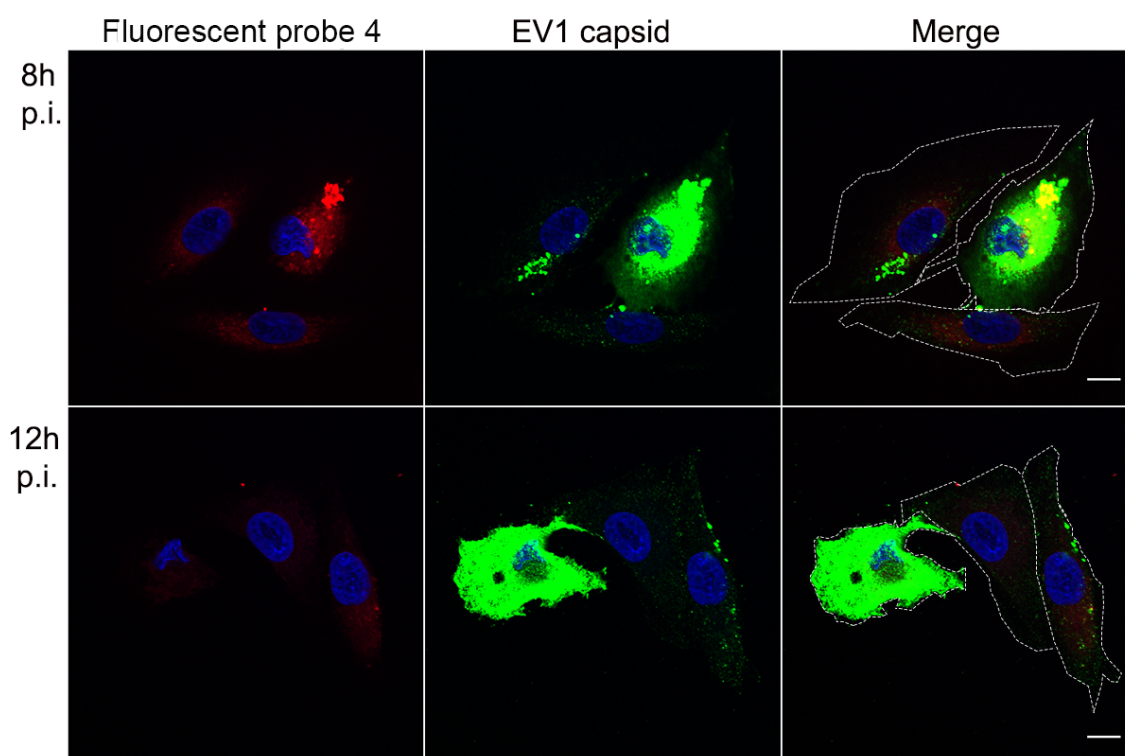


Figure S10. Fluorescent probe (4) conjugated to EV1 and internalized to cells. At 8h p.i. virus-fluorescent probe conjugate is still seen in the vesicular structures with the EV1 capsid label. At 12 h the signal is weaker. Scale bars 10 μm .

Modelling of the hydrophobic pockets

The modelling of the pockets of EV1, CVA9 and CVB3 was done using the experimentally determined structures in⁶⁻⁸. The solvent accessible volume of the pockets was analysed by using the Visual Molecular Dynamics (VMD) software (see: <http://www.ks.uiuc.edu/Research/vmd/>). The local environment around one of the 60 symmetrical pockets was taken from the full icosahedral virus particle. The free space in the pocket was modeled with solvent accessible volume method by fitting different size of probe spheres to the empty space. The minimum 1.4 Å radius of the spheres was defined to mimic the size of a water molecule. After modeling the positions of the probe spheres form a densely distributed group of points based on which analysis and visualization were made. To analyze the direct entrance into the pockets, the group of spheres was divided into 1 Å thick slices perpendicular to the direction of the entrance. For CVA9 and CVB3 the direction of the direct entrance was determined based on the positions of the probe spheres with minimum distance over the gap. The pair correlation function was calculated for each slice from which the minimum and maximum dimensions were estimated based on the behavior of the function. All the corresponding slices that were used in analysis are also shown in the

visualizations. The position of the probe molecule in the pockets was fitted by hand to the empty space described by the probe spheres. The goal was to minimize the number of regions seen outside the pocket, and on the other hand, to reach the free surface of the virus.

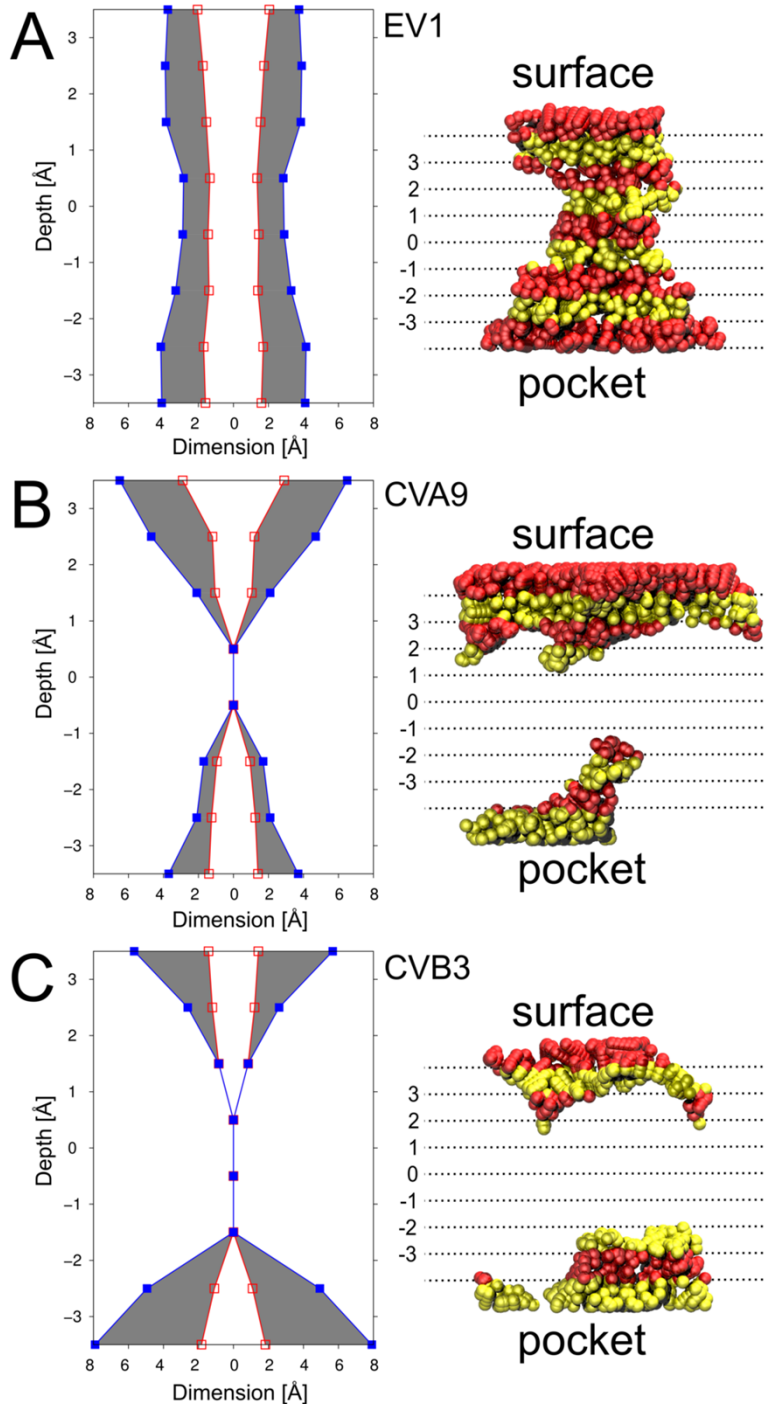


Fig S11. Dimensions of the main entrances of the pocket modelled from the experimental structures for A) EV1, B) CVA9 and C) CVB3 as described in methods section. From the probe (2) spheres used is space filling method, minimum and maximum dimensions of the pocket are estimated from the pair correlation function. The minimum (empty squares) and the maximum (filled squares) dimensions are shown on the left panel and the structure on the right panel. Structure is divided into a 1 Å thick slabs perpendicular to the direction of the main entrance.

References

- 1 R. Sauer, A. Turshatov, S. Balushev and K. Landfester, *Macromolecules*, 2012, **45**, 3787–3796.
- 2 K. Salorinne, T. Lahtinen, V. Marjomäki and H. Häkkinen, *CrystEngComm*, 2014, **16**, 9001–9009.
- 3 K. Salorinne, T. Lahtinen, S. Malola, J. Koivisto and H. Häkkinen, *Nanoscale*, 2014, **6**, 7823–6.
- 4 T. J. Sørensen, E. Thyryhaug, M. Szabelski, R. Luchowski, I. Gryczynski, Z. Gryczynski and B. W. Laursen, *Methods Appl. Fluoresc.*, 2013, **1**, 25001.
- 5 E. Thyryhaug, T. J. Sørensen, I. Gryczynski, Z. Gryczynski and B. W. Laursen, *J. Phys. Chem. A*, 2013, **117**, 2160–2168.
- 6 D. J. Filman, M. W. Wien, J. A. Cunningham, J. M. Bergelson and J. M. Hogle, *Acta Crystallogr. D. Biol. Crystallogr.*, 1998, **54**, 1261–1272.
- 7 S. Shakeel, J. J. T. Seitsonen, T. Kajander, P. Laurinmäki, T. Hyypiä, P. Susi and S. J. Butcher, *J. Virol.*, 2013, **87**, 3943–51.
- 8 J. D. Yoder, J. O. Cifuentes, J. Pan, J. M. Bergelson and S. Hafenstein, *J. Virol.*, 2012, **86**, 12571–12581.